International Tables for Crystallography (2006). Vol. B, Section 5.1.2, pp. 534–538.

5.1. Dynamical theory of X-ray diffraction

BY A. AUTHIER

5.1.1. Introduction

The first experiment on X-ray diffraction by a crystal was performed by W. Friedrich, P. Knipping and M. von Laue in 1912 and Bragg's law was derived in 1913 (Bragg, 1913). Geometrical and dynamical theories for the intensities of the diffracted X-rays were developed by Darwin (1914*a*,*b*). His dynamical theory took into account the interaction of X-rays with matter by solving recurrence equations that describe the balance of partially transmitted and partially reflected amplitudes at each lattice plane. This is the first form of the dynamical theory of X-ray diffraction. It gives correct expressions for the reflected intensities and was extended to the absorbing-crystal case by Prins (1930). A second form of dynamical theory was introduced by Ewald (1917) as a continuation of his previous work on the diffraction of optical waves by crystals. He took into account the interaction of X-rays with matter by considering the crystal to be a periodic distribution of dipoles which were excited by the incident wave. This theory also gives the correct expressions for the reflected and transmitted intensities, and it introduces the fundamental notion of a wavefield, which is necessary to understand the propagation of X-rays in perfect or deformed crystals. Ewald's theory was later modified by von Laue (1931), who showed that the interaction could be described by solving Maxwell's equations in a medium with a continuous, triply periodic distribution of dielectric susceptibility. It is this form which is most widely used today and which will be presented in this chapter.

The geometrical (or kinematical) theory, on the other hand, considers that each photon is scattered only once and that the interaction of X-rays with matter is so small it can be neglected. It can therefore be assumed that the amplitude incident on every diffraction centre inside the crystal is the same. The total diffracted amplitude is then simply obtained by adding the individual amplitudes diffracted by each diffracting centre, taking into account only the geometrical phase differences between them and neglecting the interaction of the radiation with matter. The result is that the distribution of diffracted amplitudes in reciprocal space is the Fourier transform of the distribution of diffracting centres in physical space. Following von Laue (1960), the expression *geometrical theory* will be used throughout this chapter when referring to these geometrical phase differences.

The first experimentally measured reflected intensities were not in agreement with the theoretical values obtained with the more rigorous dynamical theory, but rather with the simpler geometrical theory. The integrated reflected intensities calculated using geometrical theory are proportional to the square of the structure factor, while the corresponding expressions calculated using dynamical theory for an infinite perfect crystal are proportional to the modulus of the structure factor. The integrated intensity calculated by geometrical theory is also proportional to the volume of the crystal bathed in the incident beam. This is due to the fact that one neglects the decrease of the incident amplitude as it progresses through the crystal and a fraction of it is scattered away. According to geometrical theory, the diffracted intensity would therefore increase to infinity if the volume of the crystal was increased to infinity, which is of course absurd. The theory only works because the strength of the interaction is very weak and if it is applied to very small crystals. How small will be shown quantitatively in Sections 5.1.6.5 and 5.1.7.2. Darwin (1922) showed that it can also be applied to large imperfect crystals. This is done using the model of mosaic crystals (Bragg *et al*., 1926). For perfect or nearly perfect crystals, dynamical theory should be used. Geometrical theory presents another drawback: it gives no indication as to the phase of the reflected wave. This is due to the fact that it is based on the Fourier transform of the electron density limited by the external shape of the crystal. This is not important when one is only interested in measuring the reflected intensities. For any problem where the phase is important, as is the case for multiple reflections, interference between coherent blocks, standing waves *etc.*, dynamical theory should be used, even for thin or imperfect crystals.

Until the 1940s, the applications of dynamical theory were essentially intensity measurements. From the 1950s to the 1970s, applications were related to the properties (absorption, interference, propagation) of wavefields in perfect or nearly perfect crystals: anomalous transmission, diffraction of spherical waves, interpretation of images on X-ray topographs, accurate measurement of form factors, lattice-parameter mapping. In recent years, they have been concerned mainly with crystal optics, focusing and the design of monochromators for synchrotron radiation [see, for instance, Batterman & Bilderback (1991)], the location of atoms at crystal surfaces and interfaces using the standing-waves method [see, for instance, the reviews by Authier (1989) and Zegenhagen (1993)], attempts to determine phases using multiple reflections [see, for instance, Chang (1987) and Hümmer & Weckert (1995)], characterization of the crystal perfection of epilayers and superlattices by high-resolution diffractometry [see, for instance, Tanner (1990) and Fewster (1993)], *etc.*

For reviews of dynamical theory, see Zachariasen (1945), von Laue (1960), James (1963), Batterman & Cole (1964), Authier (1970), Kato (1974), Brümmer & Stephanik (1976), Pinsker (1978), Authier & Malgrange (1998), and Authier (2001). Topography is described in Chapter 2.7 of *IT* C (1999), in Tanner (1976) and in Tanner & Bowen (1992). For the use of Bragg-angle measurements for accurate lattice-parameter mapping, see Hart (1981).

A reminder of some basic concepts in electrodynamics is given in Section A5.1.1.1 of the Appendix.

5.1.2. Fundamentals of plane-wave dynamical theory

5.1.2.1. *Propagation equation*

The wavefunction Ψ associated with an electron or a neutron beam is *scalar* while an electromagnetic wave is a *vector* wave. When propagating in a medium, these waves are solutions of a *propagation equation*. For electrons and neutrons, this is Schrödinger's equation, which can be rewritten as

$$\Delta\Psi + 4\pi^2 k^2(1+\chi)\Psi = 0, \qquad (5.1.2.1)$$

where $k = 1/\lambda$ is the wavenumber in a vacuum, $\chi = \varphi/W$ (φ is the potential in the crystal and W is the accelerating voltage) in the case of electron diffraction and $\chi = -2mV(\mathbf{r})/h^2k^2$ [$V(\mathbf{r})$ is the Fermi pseudo-potential and h is Planck's constant] in the case of neutron diffraction. The dynamical theory of electron diffraction is treated in Chapter 5.2 [note that a different convention is used in Chapter 5.2 for the scalar wavenumber: $k = 2\pi/\lambda$; compare, for example, equation (5.2.2.1) and its equivalent, equation (5.1.2.1)] and the dynamical theory of neutron diffraction is treated in Chapter 5.3.

In the case of X-rays, the propagation equation is deduced from Maxwell's equations after neglecting the interaction with protons. Following von Laue (1931, 1960), it is assumed that the positive charge of the nuclei is distributed in such a way that the medium is everywhere locally neutral and that there is no current. As a first approximation, magnetic interaction, which is very weak, is not taken into account in this review. The propagation equation is

derived in Section A5.1.1.2 of the Appendix. Expressed in terms of the local electric displacement, $\mathbf{D}(\mathbf{r})$, it is given for monochromatic waves by

$$\Delta\mathbf{D}(\mathbf{r}) + \text{ curl curl } \chi\mathbf{D}(\mathbf{r}) + 4\pi^2k^2\mathbf{D}(\mathbf{r}) = 0. \qquad (5.1.2.2)$$

The interaction of X-rays with matter is characterized in equation (5.1.2.2) by the parameter χ, which is the dielectric susceptibility. It is classically related to the electron density $\rho(\mathbf{r})$ by

$$\chi(\mathbf{r}) = -R\lambda^2\rho(\mathbf{r})/\pi, \qquad (5.1.2.3)$$

where $R = 2.81794 \times 10^{-6}$ nm is the classical radius of the electron [see equation (A5.1.1.2) in Section A5.1.1.2 of the Appendix].

The dielectric susceptibility, being proportional to the electron density, is triply periodic in a crystal. It can therefore be expanded in Fourier series:

$$\chi = \sum_{\mathbf{h}} \chi_h \exp(2\pi i\mathbf{h}\cdot\mathbf{r}), \qquad (5.1.2.4)$$

where $\mathbf{h}$ is a reciprocal-lattice vector and the summation is extended over all reciprocal-lattice vectors. The sign convention adopted here for Fourier expansions of periodic functions is the *standard crystallographic* sign convention defined in Section 2.5.2.3. The relative orientations of wavevectors and reciprocal-lattice vectors are defined in Fig. 5.1.2.1, which represents schematically a Bragg reflection in direct and reciprocal space (Figs. 5.1.2.1*a* and 5.1.2.1*b*, respectively).

The coefficients χ_h of the Fourier expansion of the dielectric susceptibility are related to the usual structure factor F_h by

$$\chi_h = -R\lambda^2F_h/(\pi V), \qquad (5.1.2.5)$$

where V is the volume of the unit cell and the structure factor is given by

$$\begin{aligned} F_h &= \sum_j (f_j + f_j' + if_j'') \exp(-M_j - 2\pi i\mathbf{h}\cdot\mathbf{r}_j) \\ &= |F_h| \exp(i\varphi_h). \end{aligned} \qquad (5.1.2.6)$$

f_j is the form factor of atom j, f_j' and f_j'' are the dispersion corrections [see, for instance, *IT* C, Section 4.2.6] and $\exp(-M_j)$ is the Debye–Waller factor. The summation is over all the atoms in the unit cell. The phase φ_h of the structure factor depends of course on the choice of origin of the unit cell. The Fourier coefficients χ_h are dimensionless. Their order of magnitude varies from 10^{-5} to 10^{-7} depending on the wavelength and the structure factor. For example, χ_h is -9.24×10^{-6} for the 220 reflection of silicon for Cu $K\alpha$ radiation.

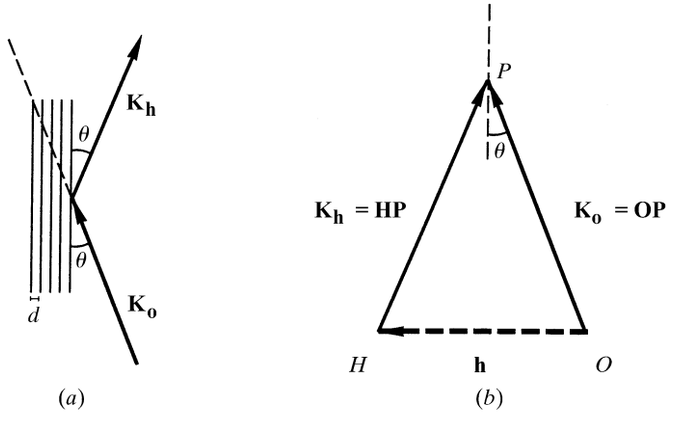

Fig. 5.1.2.1. Bragg reflection. (*a*) Direct space. Bragg reflection of a wave of wavevector $\mathbf{K_o}$ incident on a set of lattice planes of spacing d. The reflected wavevector is $\mathbf{K_h}$. Bragg's law $2d\sin\theta = n\lambda$ can also be written $2d_{hkl}\sin\theta = \lambda$, where $d_{hkl} = d/n = 1/OH = 1/h$ is the inverse of the length of the corresponding reciprocal-lattice vector $\mathbf{OH} = \mathbf{h}$ (see part *b*). (*b*) Reciprocal space. P is the tie point of the wavefield consisting of the incident wave $\mathbf{K_o} = \mathbf{OP}$ and the reflected wave $\mathbf{K_h} = \mathbf{HP}$. Note that the wavevectors are oriented *towards* the tie point.

In an absorbing crystal, absorption is taken into account phenomenologically through the imaginary parts of the index of refraction and of the wavevectors. The dielectric susceptibility is written

$$\chi = \chi_r + i\chi_i. \qquad (5.1.2.7)$$

The real and imaginary parts of the susceptibility are triply periodic in a crystalline medium and can be expanded in a Fourier series,

$$\begin{aligned} \chi_r &= \sum_{\mathbf{h}} \chi_{rh} \exp(2\pi i\mathbf{h}\cdot\mathbf{r}) \\ \chi_i &= \sum_{\mathbf{h}} \chi_{ih} \exp(2\pi i\mathbf{h}\cdot\mathbf{r}), \end{aligned} \qquad (5.1.2.8)$$

where

$$\begin{aligned} \chi_{rh} &= -R\lambda^2F_{rh}/(\pi V), \\ \chi_{ih} &= -R\lambda^2F_{ih}/(\pi V) \end{aligned} \qquad (5.1.2.9)$$

and

$$\begin{aligned} F_{rh} &= \sum_j (f_j + f_j') \exp(-M_j - 2\pi i\mathbf{h}\cdot\mathbf{r}_j) \\ &= |F_{rh}| \exp(i\varphi_{rh}), \qquad (5.1.2.10a) \\ F_{ih} &= \sum_j (f_j'') \exp(-M_j - 2\pi i\mathbf{h}\cdot\mathbf{r}_j) \\ &= |F_{ih}| \exp(i\varphi_{ih}). \qquad (5.1.2.10b) \end{aligned}$$

It is important to note that

$$F_{rh}^* = F_{r\bar{h}} \text{ and } F_{ih}^* = F_{i\bar{h}} \text{ but that } F_h^* \neq F_{\bar{h}}, \qquad (5.1.2.11)$$

where f^* is the imaginary conjugate of f.

The *index of refraction* of the medium for X-rays is

$$n = 1 + \chi_{ro}/2 = 1 - R\lambda^2F_o/(2\pi V), \qquad (5.1.2.12)$$

where F_o/V is the number of electrons per unit volume. This index is very slightly smaller than one. It is for this reason that specular reflection of X-rays takes place at grazing angles. From the value of the critical angle, $(-\chi_{ro})^{1/2}$, the electron density F_o/V of a material can be determined.

The linear absorption coefficient is

$$\mu_o = -2\pi k\chi_{io} = 2R\lambda F_{io}/V. \qquad (5.1.2.13)$$

For example, it is 143.2 cm^{-1} for silicon and Cu $K\alpha$ radiation.

5.1.2.2. *Wavefields*

The notion of a wavefield, introduced by Ewald (1917), is one of the most fundamental concepts in dynamical theory. It results from the fact that since the propagation equation (5.1.2.2) is a second-order partial differential equation with a periodic interaction coefficient, its solution has the same periodicity,

$$\mathbf{D} = \exp(-2\pi i\mathbf{K_o}\cdot\mathbf{r}) \sum_{\mathbf{h}} \mathbf{D_h} \exp(2\pi i\mathbf{h}\cdot\mathbf{r}), \qquad (5.1.2.14)$$

where the summation is over all reciprocal-lattice vectors $\mathbf{h}$. Equation (5.1.2.14) can also be written

$$\mathbf{D} = \sum_{\mathbf{h}} \mathbf{D_h} \exp(-2\pi i\mathbf{K_h}\cdot\mathbf{r}), \qquad (5.1.2.15)$$

where

$$\mathbf{K_h} = \mathbf{K_o} - \mathbf{h}. \qquad (5.1.2.16)$$

Expression (5.1.2.15) shows that the solution of the propagation equation can be interpreted as an infinite sum of plane waves with amplitudes $\mathbf{D_h}$ and wavevectors $\mathbf{K_h}$. This sum is a *wavefield*, or *Ewald wave*. The same expression is used to describe the propagation of any wave in a periodic medium, such as phonons or electrons in a solid. Expression (5.1.2.14) was later called a *Bloch wave* by solid-state physicists.

The wavevectors in a wavefield are deduced from one another by translations of the reciprocal lattice [expression (5.1.2.16)]. They can be represented geometrically as shown in Fig. 5.1.2.1(*b*). The wavevectors $\mathbf{K_o} = \mathbf{OP}$; $\mathbf{K_h} = \mathbf{HP}$ are drawn *away* from reciprocal-lattice points. Their common extremity, *P*, called the *tie point* by Ewald, characterizes the wavefield.

In an absorbing crystal, wavevectors have an imaginary part,

$$\mathbf{K_o} = \mathbf{K}_{or} + i\mathbf{K}_{oi};\ \ \mathbf{K_h} = \mathbf{K}_{hr} + i\mathbf{K}_{hi},$$

and (5.1.2.16) shows that all wavevectors have the same imaginary part,

$$\mathbf{K}_{oi} = \mathbf{K}_{hi}, \qquad (5.1.2.17)$$

and therefore undergo the same absorption. This is one of the most important properties of wavefields.

5.1.2.3. *Boundary conditions at the entrance surface*

The choice of the '**o**' component of expansion (5.1.2.15) is arbitrary in an infinite medium. In a semi-infinite medium where the waves are created at the interface with a vacuum or air by an incident plane wave with wavevector $\mathbf{K}_\mathbf{o}^{(a)}$ (using von Laue's notation), the choice of $\mathbf{K_o}$ is determined by the boundary conditions.

This condition for wavevectors at an interface demands that their tangential components should be continuous across the boundary, in agreement with Descartes–Snell's law. This condition is satisfied when the difference between the wavevectors on each side of the interface is parallel to the normal to the interface. This is shown geometrically in Fig. 5.1.2.2 and formally in (5.1.2.18):

$$\mathbf{K_o} - \mathbf{K}_\mathbf{o}^{(a)} = \mathbf{OP} - \mathbf{OM} = \overline{MP} \cdot \mathbf{n}, \qquad (5.1.2.18)$$

where $\mathbf{n}$ is a unit vector normal to the crystal surface, oriented towards the inside of the crystal.

There is no absorption in a vacuum and the incident wavevector $\mathbf{K}_\mathbf{o}^{(a)}$ is real. Equation (5.1.2.18) shows that it is the component normal to the interface of wavevector $\mathbf{K_o}$ which has an imaginary part,

$$\mathbf{K}_{oi} = \mathcal{I}(\overline{MP}) \cdot \mathbf{n} = -\mu\mathbf{n}/(4\pi\gamma_o), \qquad (5.1.2.19)$$

where $\mathcal{I}(f)$ is the imaginary part of f, $\gamma_o = \cos(\mathbf{n} \cdot \mathbf{s_o})$ and $\mathbf{s_o}$ is a unit vector in the incident direction. When there is more than one wave in the wavefield, the effective absorption coefficient μ can differ significantly from the normal value, μ_o, given by (5.1.2.13) – see Section 5.1.5.

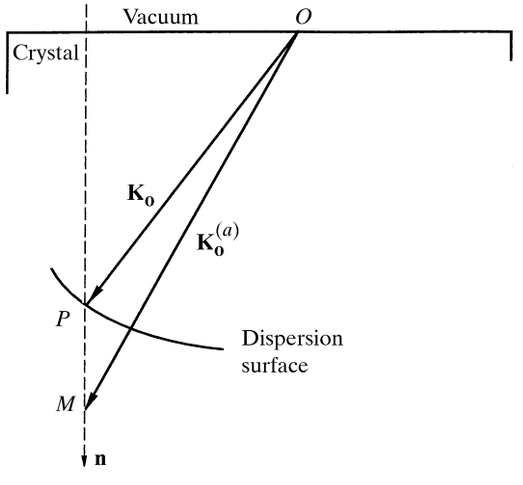

Fig. 5.1.2.2. Boundary condition for wavevectors at the entrance surface of the crystal.

5.1.2.4. *Fundamental equations of dynamical theory*

In order to obtain the solution of dynamical theory, one inserts expansions (5.1.2.15) and (5.1.2.4) into the propagation equation (5.1.2.2). This leads to an equation with an infinite sum of terms. It is shown to be equivalent to an infinite system of linear equations which are the *fundamental equations* of dynamical theory. Only those terms in (5.1.2.15) whose wavevector magnitudes K_h are very close to the vacuum value, k, have a non-negligible amplitude. These wavevectors are associated with reciprocal-lattice points that lie very close to the Ewald sphere. Far from any Bragg reflection, their number is equal to 1 and a single plane wave propagates through the medium. In general, for X-rays, there are only two reciprocal-lattice points on the Ewald sphere. This is the so-called *two-beam* case to which this treatment is limited. There are, however, many instances where several reciprocal-lattice points lie simultaneously on the Ewald sphere. This corresponds to the *many-beam* case which has interesting applications for the determination of phases of reflections [see, for instance, Chang (1987) and Hümmer & Weckert (1995)]. On the other hand, for electrons, there are in general many reciprocal-lattice points close to the Ewald sphere and many wavefields are excited simultaneously (see Chapter 5.2).

In the two-beam case, for reflections that are not highly asymmetric and for Bragg angles that are not close to $\pi/2$, the fundamental equations of dynamical theory reduce to

$$\begin{aligned} 2X_oD_o - kC\chi_{\bar{h}}D_h &= 0 \\ -kC\chi_hD_o + 2X_hD_h &= 0, \end{aligned} \qquad (5.1.2.20)$$

where $C = 1$ if $\mathbf{D_h}$ is normal to the $\mathbf{K_o}, \mathbf{K_h}$ plane and $C = \cos 2\theta$ if $\mathbf{D_h}$ lies in the plane; this is due to the fact that the amplitude with which electromagnetic radiation is scattered is proportional to the sine of the angle between the direction of the electric vector of the incident radiation and the direction of scattering (see, for instance, *IT* C, Section 6.2.2). The polarization of an electromagnetic wave is classically related to the orientation of the electric vector; in dynamical theory it is that of the electric displacement which is considered (see Section A5.1.1.3 of the Appendix).

The system (5.1.2.20) is therefore a system of four equations which admits four solutions, two for each direction of polarization. In the *non-absorbing* case, to a very good approximation,

$$\begin{aligned} X_o &= K_o - nk, \\ X_h &= K_h - nk. \end{aligned} \qquad (5.1.2.21)$$

In the case of an *absorbing crystal*, X_o and K_h are complex. Equation (5.1.5.2) gives the full expression for X_o.

5.1.2.5. *Dispersion surface*

The fundamental equations (5.1.2.20) of dynamical theory are a set of linear homogeneous equations whose unknowns are the amplitudes of the various waves which make up a wavefield. For the solution to be non-trivial, the determinant of the set must be set equal to zero. This provides a secular equation relating the magnitudes of the wavevectors of a given wavefield. This equation is that of the locus of the tie points of all the wavefields that may

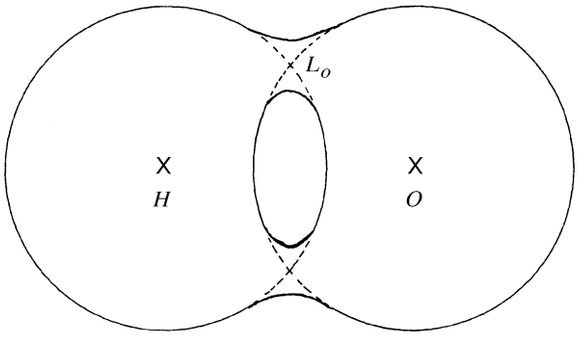

Fig. 5.1.2.3. Intersection of the dispersion surface with the plane of incidence. The dispersion surface is a connecting surface between the two spheres centred at reciprocal-lattice points O and H and with radius nk. L_o is the Lorentz point.

propagate in the crystal with a given frequency. This locus is called the *dispersion surface*. It is a constant-energy surface and is the equivalent of the index surface in optics. It is the X-ray analogue of the constant-energy surfaces known as Fermi surfaces in the electron band theory of solids.

In the two-beam case, the dispersion surface is a surface of revolution around the diffraction vector **OH**. It is made from two spheres and a connecting surface between them. The two spheres are centred at O and H and have the same radius, nk. Fig. 5.1.2.3 shows the intersection of the dispersion surface with a plane passing through **OH**. When the tie point lies on one of the two spheres, far from their intersection, only one wavefield propagates inside the crystal. When it lies on the connecting surface, two waves are excited simultaneously. The equation of this surface is obtained by equating to zero the determinant of system (5.1.2.20):

$$X_o X_h = k^2 C^2 \chi_h \chi_{\bar{h}}/4. \qquad (5.1.2.22)$$

Equations (5.1.2.21) show that, in the zero-absorption case, X_o and X_h are to be interpreted as the distances of the tie point P from the spheres centred at O and H, respectively. From (5.1.2.20) it can be seen that they are of the order of the vacuum wavenumber times the Fourier coefficient of the dielectric susceptibility, that is five or six orders of magnitude smaller than k. The two spheres can therefore be replaced by their tangential planes. Equation (5.1.2.22) shows that the product of the distances of the tie point from these planes is constant. The intersection of the dispersion surface with the plane passing through **OH** is therefore a hyperbola (Fig. 5.1.2.4) whose diameter [using (5.1.2.5) and (5.1.2.22)] is

$$\overline{A_{o2}A_{o1}} = |C|R\lambda(F_h F_{\bar{h}})^{1/2}/(\pi V \cos\theta). \qquad (5.1.2.23)$$

It can be noted that the larger the diameter of the dispersion surface, the larger the structure factor, that is, the stronger the interaction of the waves with the matter. When the polarization is parallel to the plane of incidence ($C = \cos 2\theta$), the interaction is weaker.

The asymptotes T_o and T_h to the hyperbola are tangents to the circles centred at O and H, respectively. Their intersection, L_o, is called the *Lorentz point* (Fig. 5.1.2.4).

A wavefield propagating in the crystal is characterized by a tie point P on the dispersion surface and two waves with wavevectors $\mathbf{K_o} = \mathbf{OP}$ and $\mathbf{K_h} = \mathbf{HP}$, respectively. The ratio, ξ, of their amplitudes D_h and D_o is given by means of (5.1.2.20):

$$\xi = \frac{D_h}{D_o} = \frac{2X_o}{kC\chi_{\bar{h}}} = \frac{-2\pi V X_o}{R\lambda C F_{\bar{h}}}. \qquad (5.1.2.24)$$

The hyperbola has two branches, 1 and 2, for each direction of polarization, that is, for $C = 1$ or $\cos 2\theta$ (Fig. 5.1.2.5). Branch 2 is

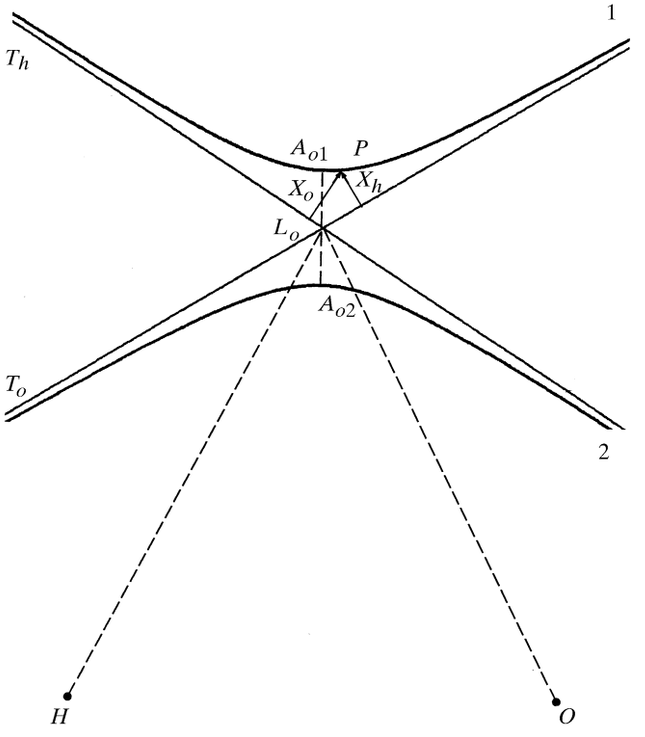

Fig. 5.1.2.4. Intersection of the dispersion surface with the plane of incidence shown in greater detail. The Lorentz point L_o is far away from the nodes O and H of the reciprocal lattice: $OL_o = HL_o = 1/\lambda$ is about 10^5 to 10^6 times larger than the diameter $A_{o1}A_{o2}$ of the dispersion surface.

the one situated on the same side of the asymptotes as the reciprocal-lattice points O and H. Given the orientation of the wavevectors, which has been chosen away from the reciprocal-lattice points (Fig. 5.1.2.1*b*), the coordinates of the tie point, X_o and X_h, are positive for branch 1 and negative for branch 2. The phase of ξ is therefore equal to $\pi + \varphi_h$ and to φ_h for the two branches, respectively, where φ_h is the phase of the structure factor [equation (5.1.2.6)]. This difference of π between the two branches has important consequences for the properties of the wavefields.

As mentioned above, owing to absorption, wavevectors are actually complex and so is the dispersion surface.

5.1.2.6. *Propagation direction*

The energy of all the waves in a given wavefield propagates in a common direction, which is obtained by calculating either the group velocity or the Poynting vector [see Section A5.1.1.4, equation (A5.1.1.8) of the Appendix]. It can be shown that, averaged over time and the unit cell, the Poynting vector of a wavefield is

$$\mathbf{S} = (c/\varepsilon_0)\exp(4\pi\mathbf{K_{oi}}\cdot\mathbf{r})\left[|D_o|^2\mathbf{s_o} + |D_h|^2\mathbf{s_h}\right], \qquad (5.1.2.25)$$

where $\mathbf{s_o}$ and $\mathbf{s_h}$ are unit vectors in the $\mathbf{K_o}$ and $\mathbf{K_h}$ directions, respectively, c is the velocity of light and ε_0 is the dielectric permittivity of a vacuum. This result was first shown by von Laue (1952) in the two-beam case and was generalized to the n-beam case by Kato (1958).

From (5.1.2.25) and equation (5.1.2.22) of the dispersion surface, it can be shown that the propagation direction of the wavefield lies along the normal to the dispersion surface at the tie point (Fig. 5.1.2.5). This result is also obtained by considering the group velocity of the wavefield (Ewald, 1958; Wagner, 1959). The angle α

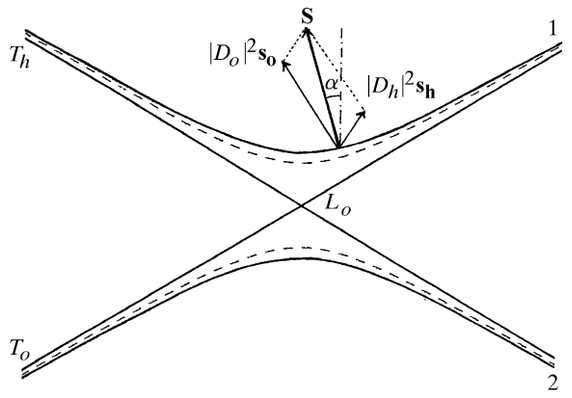

Fig. 5.1.2.5. Dispersion surface for the two states of polarization. Solid curve: polarization normal to the plane of incidence ($C = 1$); broken curve: polarization parallel to the plane of incidence ($C = \cos 2\theta$). The direction of propagation of the energy of the wavefields is along the Poynting vector, **S**, normal to the dispersion surface.

between the propagation direction and the lattice planes is given by

$$\tan\alpha = \left[(1 - |\xi|^2)/(1 + |\xi|^2)\right] \tan\theta. \qquad (5.1.2.26)$$

It should be noted that the propagation direction varies between $\mathbf{K_o}$ and $\mathbf{K_h}$ for both branches of the dispersion surface.

5.1.3. Solutions of plane-wave dynamical theory

5.1.3.1. *Departure from Bragg's law of the incident wave*

The wavefields excited in the crystal by the incident wave are determined by applying the boundary condition mentioned above for the continuity of the tangential component of the wavevectors (Section 5.1.2.3). Waves propagating in a vacuum have wavenumber $k = 1/\lambda$. Depending on whether they propagate in the incident or in the reflected direction, the common extremity, M, of their wavevectors

$$\mathbf{OM} = \mathbf{K_o^{(a)}} \text{ and } \mathbf{HM} = \mathbf{K_h^{(a)}}$$

lies on spheres of radius k and centred at O and H, respectively. The intersections of these spheres with the plane of incidence are two circles which can be approximated by their tangents T_o' and T_h' at their intersection point, L_a, or *Laue point* (Fig. 5.1.3.1).

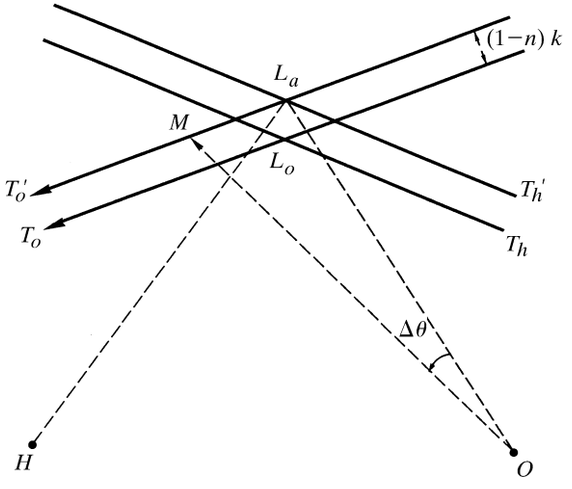

Fig. 5.1.3.1. Departure from Bragg's law of an incident wave.

Bragg's condition is exactly satisfied according to the geometrical theory of diffraction when M lies at L_a. The departure $\Delta\theta$ from Bragg's incidence of an incident wave is defined as the angle between the corresponding wavevectors **OM** and $\mathbf{OL}_a$. As $\Delta\theta$ is very small compared to the Bragg angle in the general case of X-rays or neutrons, one may write

$$\begin{aligned} \mathbf{K_o^{(a)}} &= \mathbf{OM} = \mathbf{OL}_a + \mathbf{L}_a\mathbf{M}, \\ \Delta\theta &= \overline{L_aM}/k. \end{aligned} \qquad (5.1.3.1)$$

The tangent T_o' is oriented in such a way that $\Delta\theta$ is negative when the angle of incidence is smaller than the Bragg angle.

5.1.3.2. *Transmission and reflection geometries*

The boundary condition for the continuity of the tangential component of the wavevectors is applied by drawing from M a line, **Mz**, parallel to the normal **n** to the crystal surface. The tie points of the wavefields excited in the crystal by the incident wave are at the intersections of this line with the dispersion surface. Two different situations may occur:

(*a*) *Transmission, or Laue case* (Fig. 5.1.3.2). The normal to the crystal surface drawn from M intersects *both* branches of the dispersion surface (Fig. 5.1.3.2*a*). The reflected wave is then directed towards the *inside* of the crystal (Fig. 5.1.3.2*b*). Let γ_o and γ_h be the cosines of the angles between the normal to the crystal surface, **n**, and the incident and reflected directions, respectively:

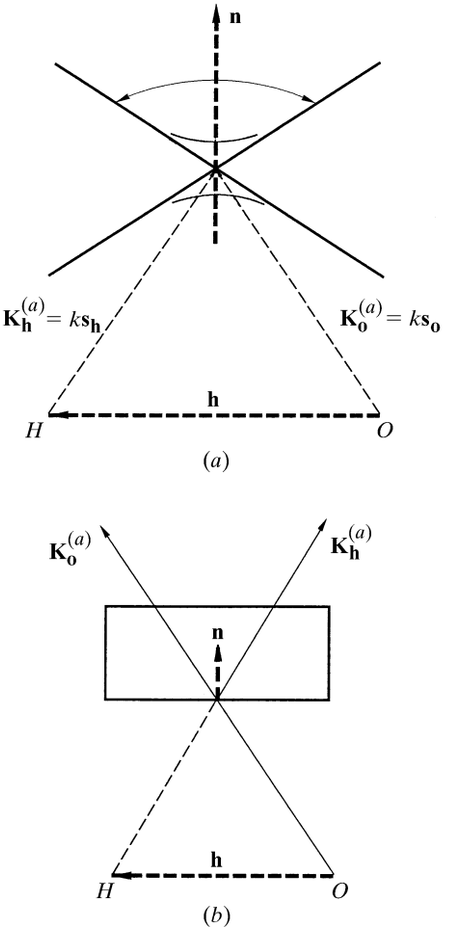

Fig. 5.1.3.2. Transmission, or Laue, geometry. (*a*) Reciprocal space; (*b*) direct space.

references